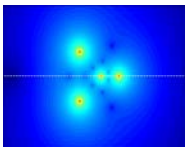

- Course 3 :
  - **Bragg with gain/loss (complex ε) modulation**
  - Unidirectionality of plane-wave coupling
  - History of gain-modulation (1970's & 1990's)
  - Kulishov's proposals :
    single-sided mirrors, strange cavities, memories
  - WGM lasers
  - Fano & EIT

Another view of modulation : scattering

- Band & coupling picture

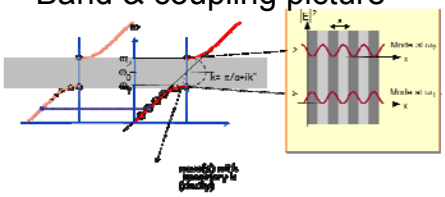

- Scattering picture [1] real index

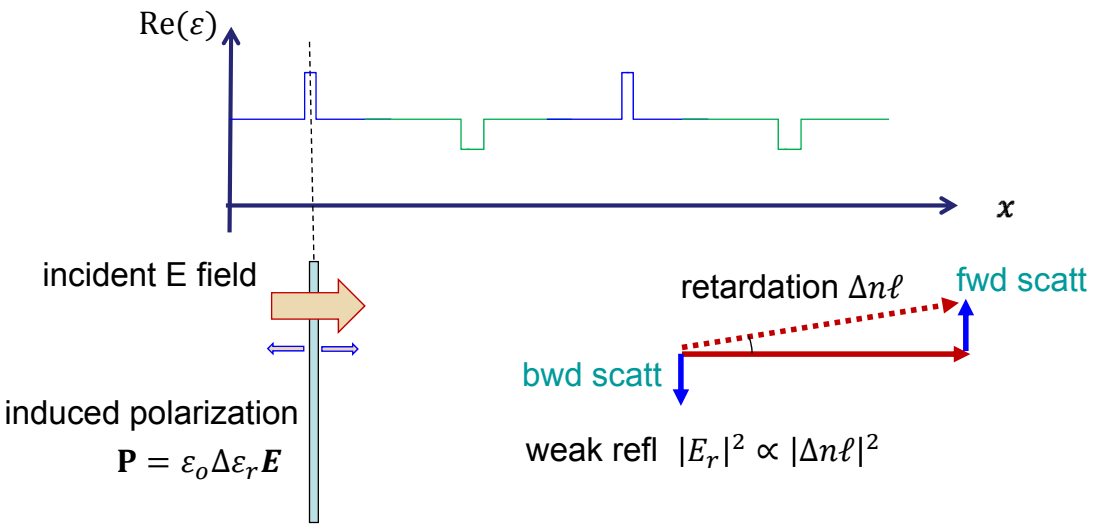

Another view of modulation : scattering

- Band & coupling picture

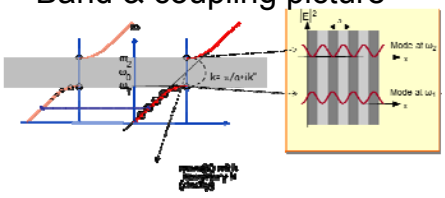

- Scattering picture [1] real index…. Second half period

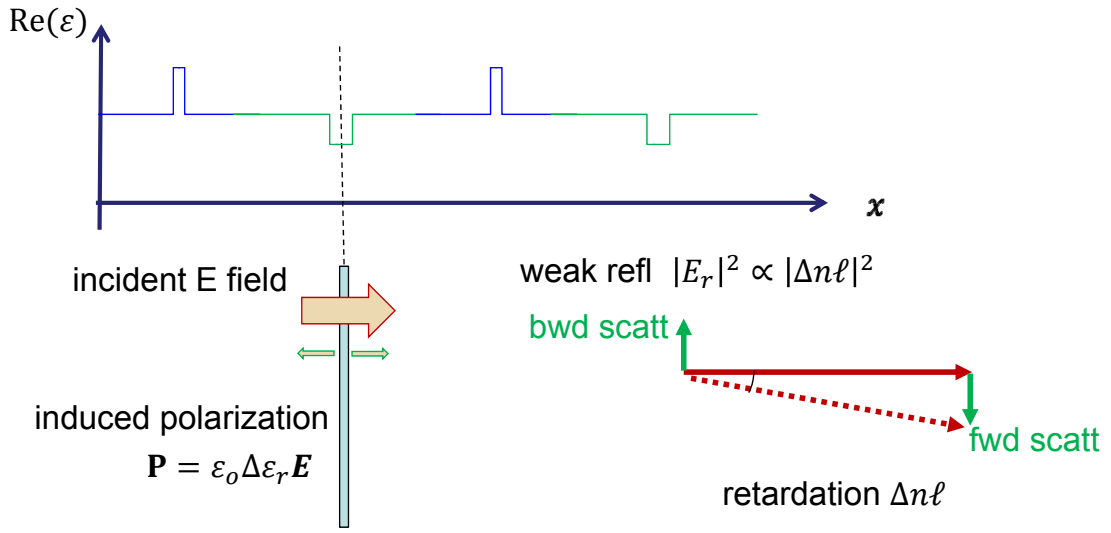

Scattering and Bragg

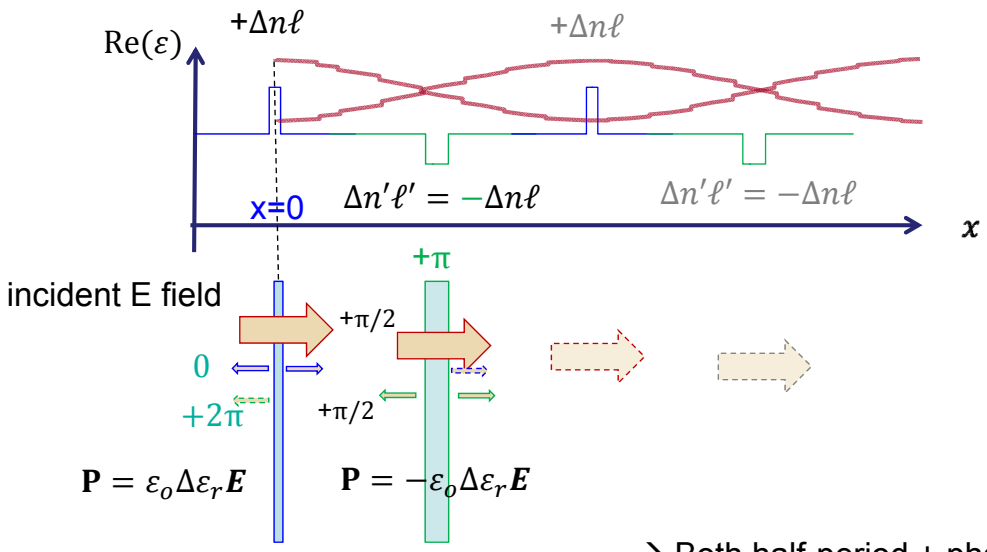

→ Both half-period + phase ref @ x=0

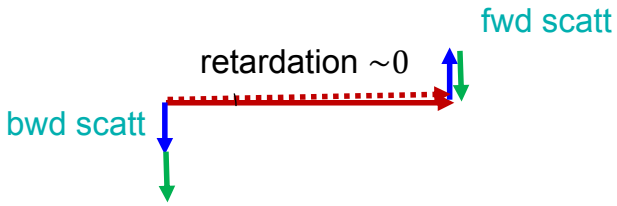

4 × weak refl $|E_r|^2 \propto 4|\Delta n\ell|^2$

Scattering and Bragg (real part)

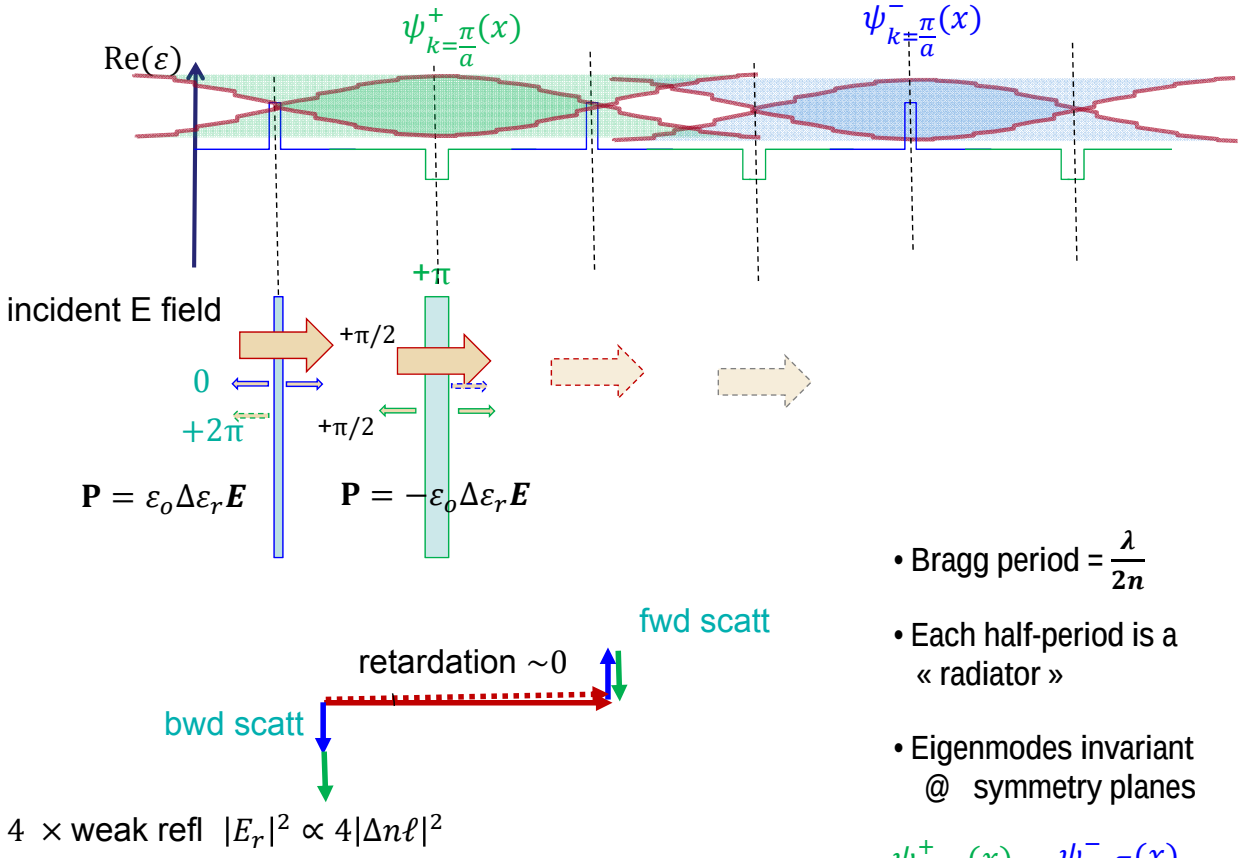

4 × weak refl $|E_r|^2 \propto 4|\Delta n \ell|^2$

- Bragg period = $\frac{\lambda}{2n}$
- Each half-period is a « radiator »
- Eigenmodes invariant @ symmetry planes

$\psi^{+}_{k=\frac{\pi}{a}}(x)$ $\psi^{-}_{k=\frac{\pi}{a}}(x)$

Another view of modulation : scattering of abs/gain layer

- Scattering picture: [2] imaginary index

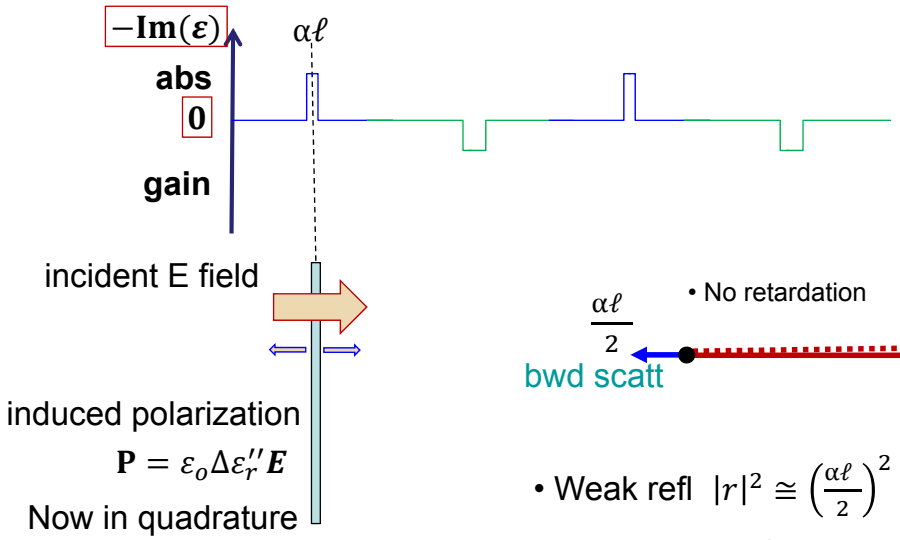

- Weak refl $|r|^2 \cong \left(\frac{\alpha\ell}{2}\right)^2$
- Attenuation $|t|^2 = 1 - \alpha\ell \cong \left(1 - \frac{\alpha\ell}{2}\right)^2$

Bragg scattering of abs/gain layers

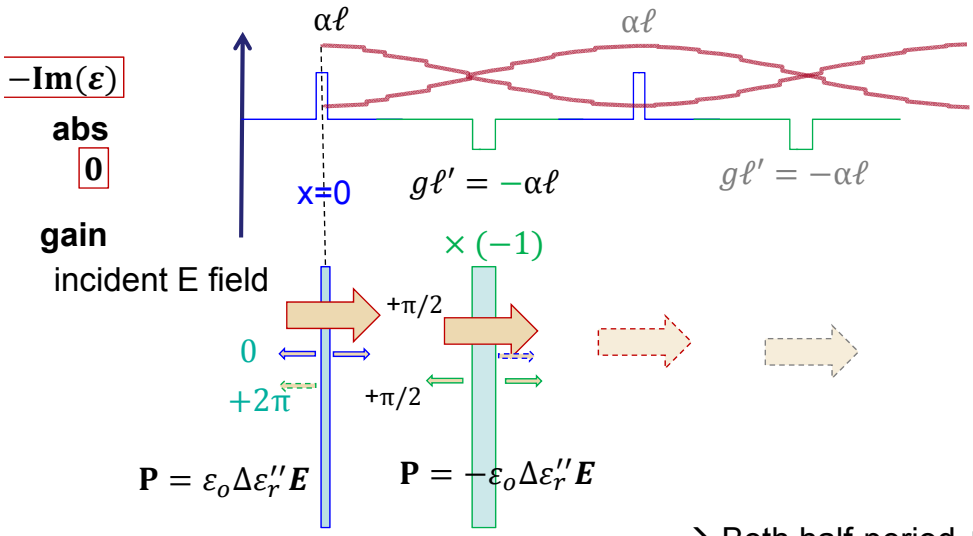

→ Both half-period + phase ref @ x=0

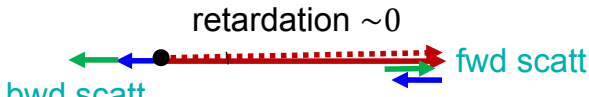

- Weak refl $|r|^2 \cong (\alpha\ell)^2$
- ~No Attenuation (gain loss compensation)

Comparison of Re and Im scattering

- |t| ~1 @ 1st order,
- Only phase of r changes

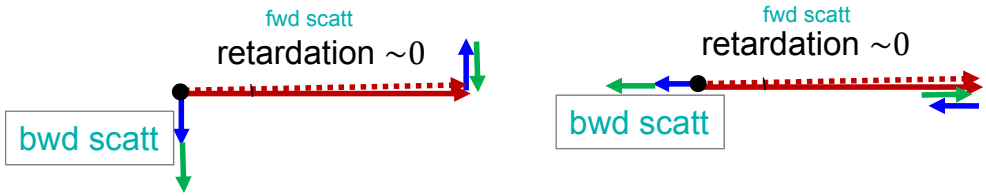

… What if we devise some clever combination ???

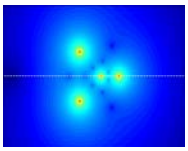

- Course 3 :
  - Bragg with gain/loss (complex ε) modulation
  - **Unidirectionality of plane-wave coupling**
  - History of gain-modulation (1970's & 1990's)
  - Kulishov's proposals :
    single-sided mirrors, strange cavities, memories
  - WGM lasers
  - Fano & EIT

One-sided cancellation of Re and Im scattering

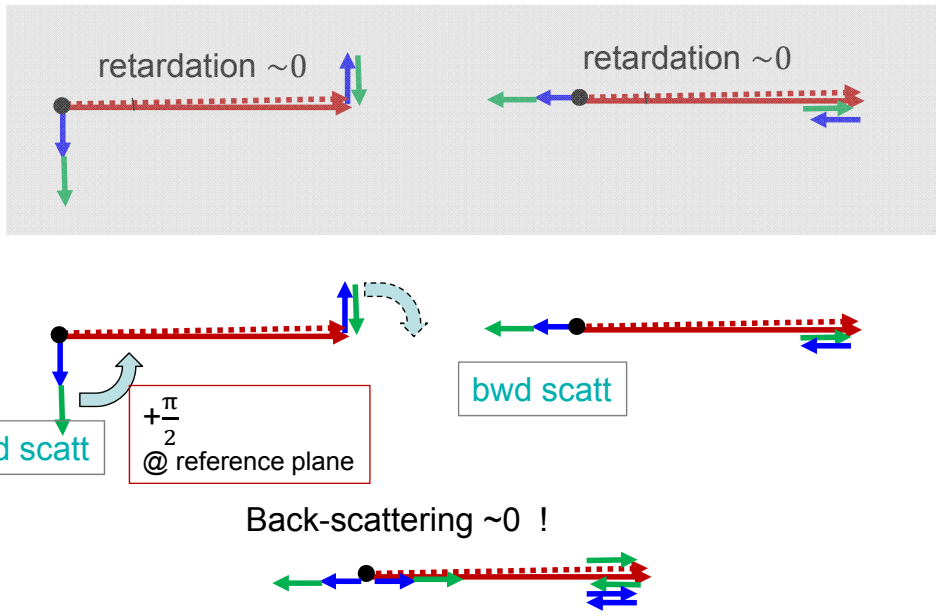

« Single-sided scattering »

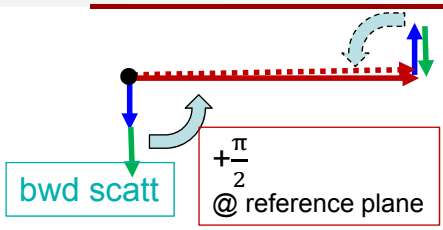

$\equiv +\frac{\pi}{4}$ by position shift & round-trip

$\equiv +\frac{\lambda}{8}$ Position shift

Back-scattering ~0 !

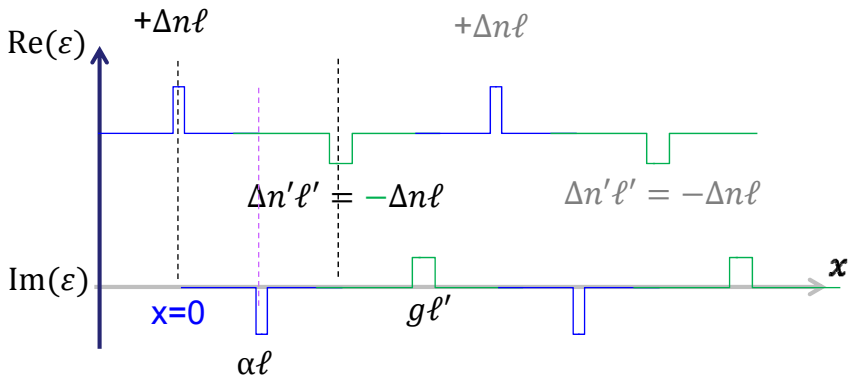

« Single-sided scattering »

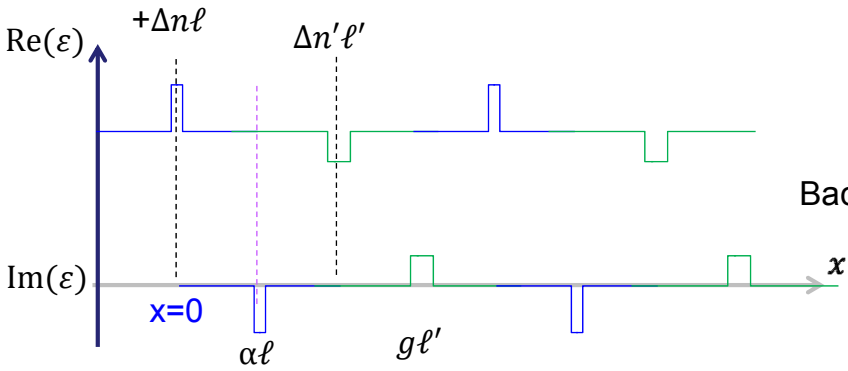

Back-scattering **cancellation**

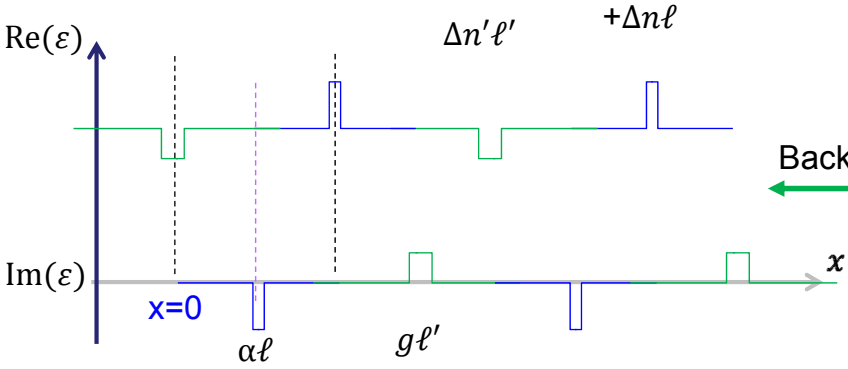

Back-scattering **enhancement**

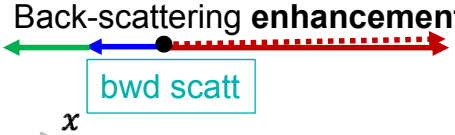

« Single-sided scattering » in Fourier language

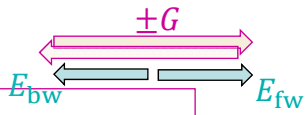

• Usual coupling constant of index grating:

$$\kappa_G \equiv < E_{\mathrm{fw}} | \Delta\varepsilon(x) | E_{\mathrm{bw}} > = \int e^{-\frac{iGx}{2}} \widehat{\Delta\varepsilon}_G \cos(Gx)\, e^{-\frac{iGx}{2}}\, dx \equiv (\tfrac{1}{2})\widehat{\Delta\varepsilon}_G$$

Hence same $\pm G$ coupling, $\kappa_G = \kappa_{-G}$

• In more generality, coupling is complex but …

$$\kappa_{\pm G} \equiv < E_{\mathrm{bw}} | \Delta\varepsilon(x) | E_{\mathrm{fw}} > = \int e^{\pm\frac{iGx}{2}} \widehat{\Delta\varepsilon}_G \cos(Gx+\varphi)\, e^{\pm\frac{iGx}{2}}\, dx = (\tfrac{1}{2})\widehat{\Delta\varepsilon}_G e^{\mp i\varphi}$$

phase here only means *shift* of grating position – usual Fourier manipulation

• Single sided band means :

$$\kappa_{+G} = \int e^{-\frac{iGx}{2}} \widehat{\Delta\varepsilon}_G (\cos Gx + i \sin Gx)\, e^{-\frac{iGx}{2}}\, dx = \int e^{-\frac{iGx}{2}} \widehat{\Delta\varepsilon}_G e^{+iGx} e^{-\frac{iGx}{2}} dx = \widehat{\Delta\varepsilon}_G$$

• But

$$\kappa_{-G} = \int e^{-\frac{iGx}{2}} \widehat{\Delta\varepsilon}_G (\cos Gx - i \sin Gx)\, e^{-\frac{iGx}{2}}\, dx = \int e^{-\frac{iGx}{2}} \widehat{\Delta\varepsilon}_G e^{-iGx} e^{-\frac{iGx}{2}} dx = 0$$

This is PT symmetry … in the basic case

What about PT symmetry …

• In our basic implementation

$\mathrm{Re}(\varepsilon)$ is symmetric and $\mathrm{Im}(\varepsilon)$ antisymmetric

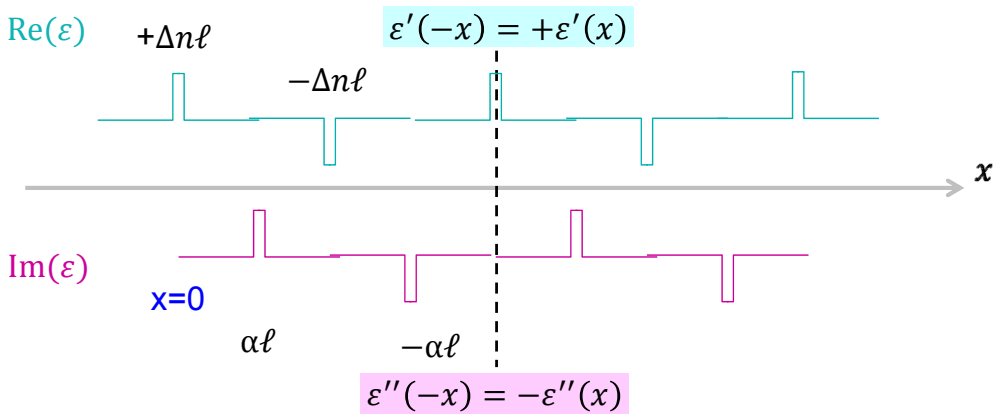

This is PT symmetry … in more general case

What about PT symmetry …

• In a more general case

Think of same Fourier rules as for signal processing

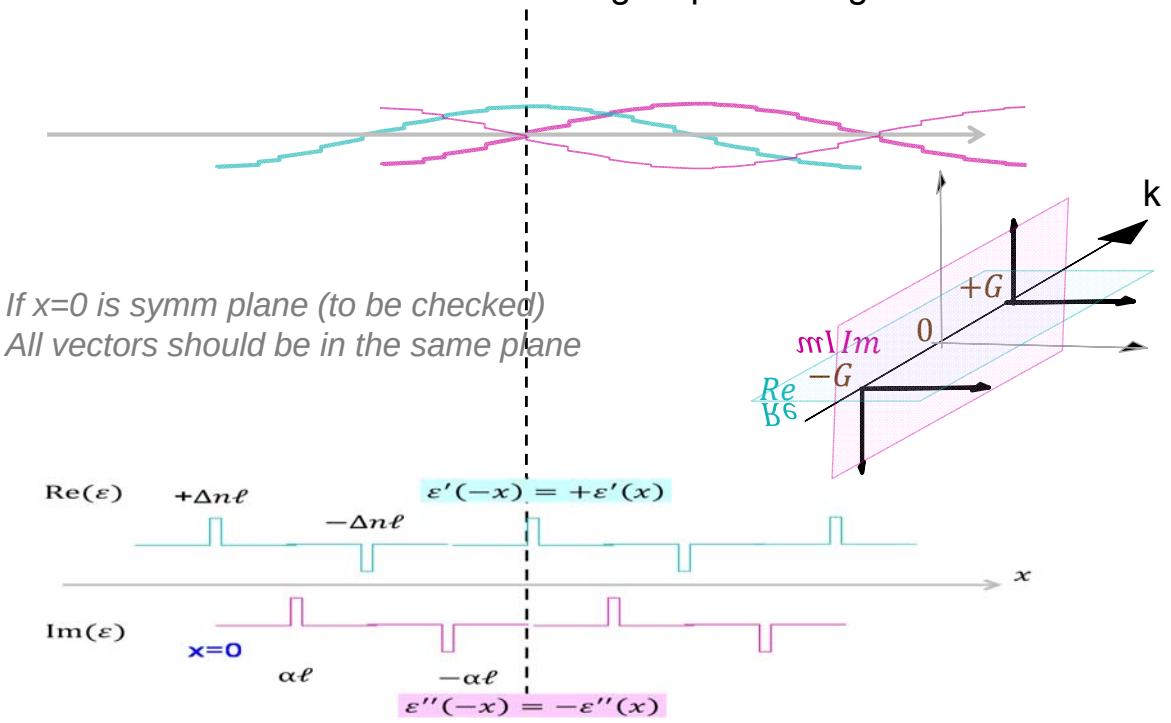

If x=0 is symm plane (to be checked)

All vectors should be in the same plane

This is PT symmetry … broken or not ?

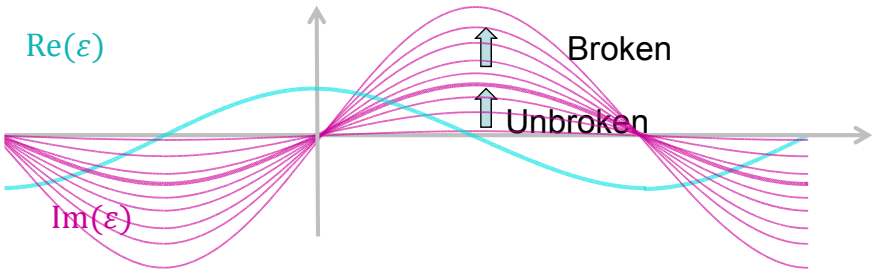

$\boldsymbol{T = 1}$ (since $\boldsymbol{R = 0}$ from on side) at Bragg frequency ?

→ only for exact balance of **Re** and ***Im*** (cf. scattering picture).

→ This is fully analogous to the case of merging eigenvalues

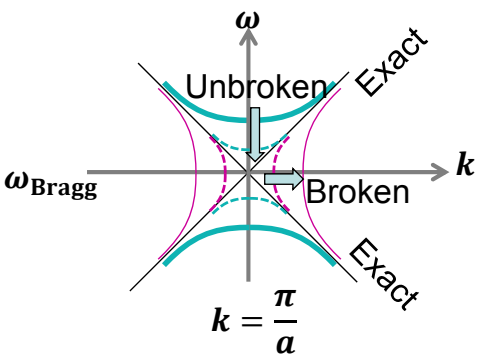

Behaviour expected around symmetry-breaking point

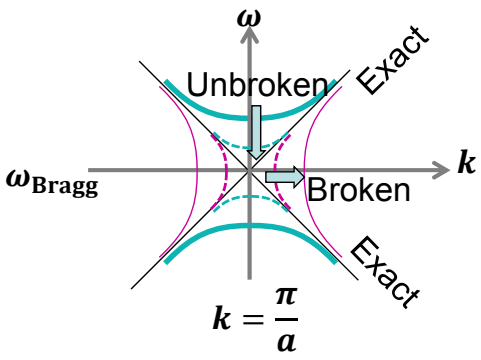

- From dip to peak in $T(\omega)$
- Passing through Rzero(one side) or Rmax (other side) $v_g(\omega)$
- Changes in group velocity $v_g(\omega)$

« Single-sided scattering » in (radio) Fourier language

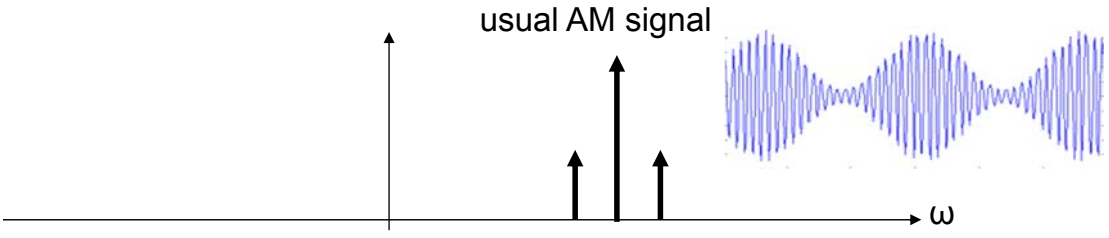

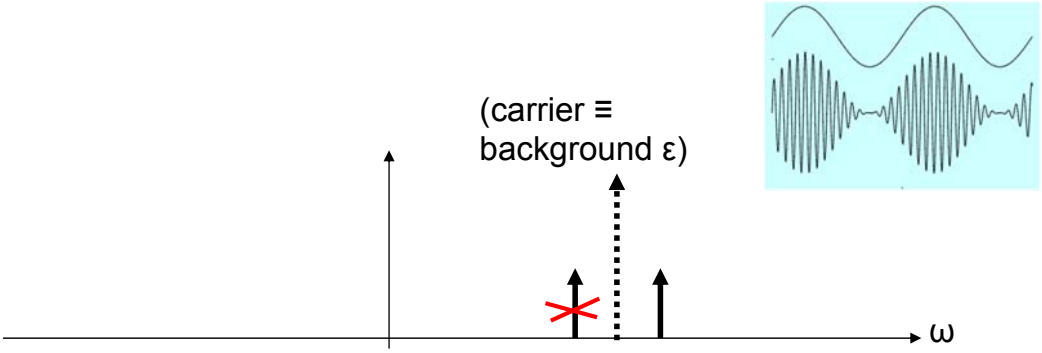

Single-side band signal
(no redundant energy)
(beating like)

Practical implementation

- Requires four different layers in layered materials

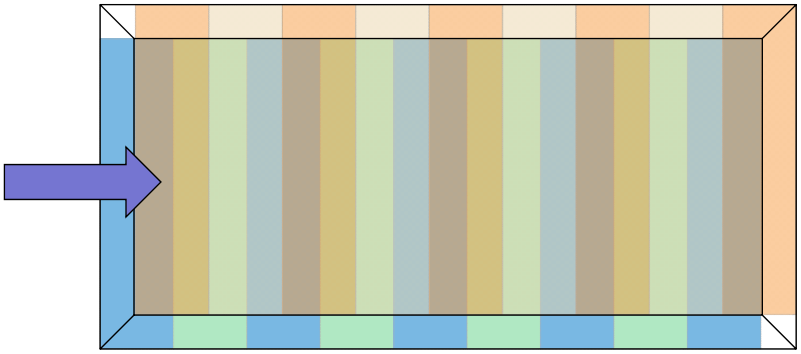

- … or two different gratings

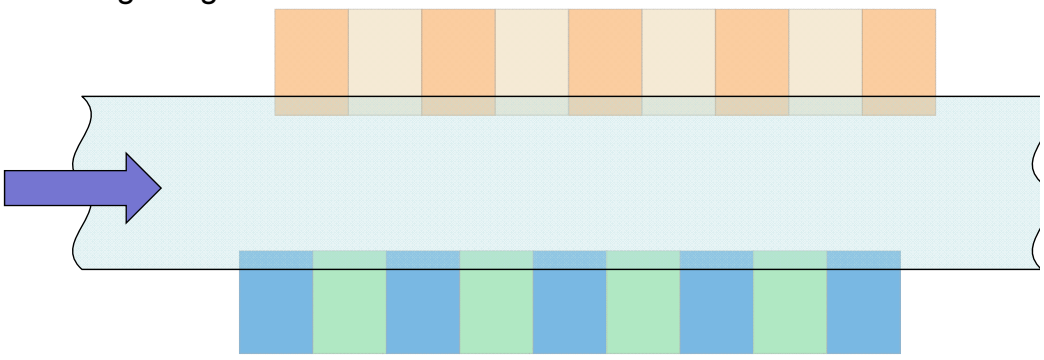

- … possible a « shape » and a « material » grating (for Re and Im resp.)

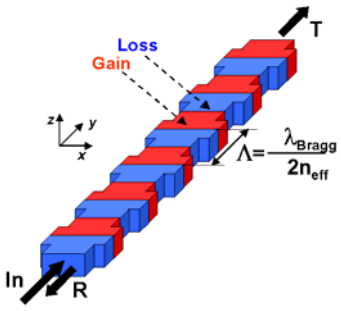

Practical implementation with tolerances

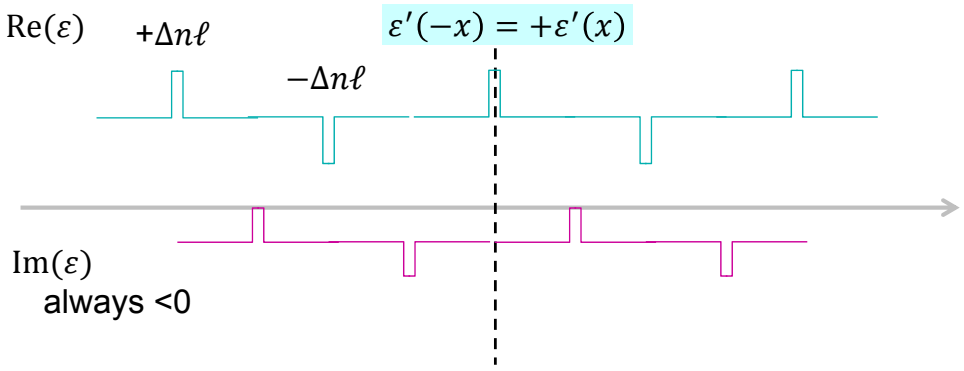

All ideal PT-Sym systems can be multiplied by
$\exp(-\langle \text{average loss} \rangle z)$ to lower $\mathrm{Im}(\varepsilon)$ in negative-only territory

(~ "Passive PT systems")

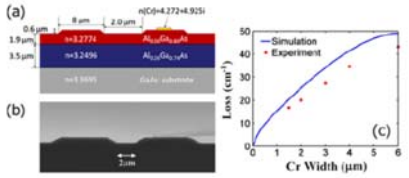

FIG. 3 (color online). Non-Hermitian dual structure. (a) Design details and complex refractive index distribution. (b) Scanning electron microscopy picture of the finalized passive $\mathcal{PT}$ device with the Cr stripe shown on the right. (c) Modal loss of isolated waveguide structure as a function of Cr width.

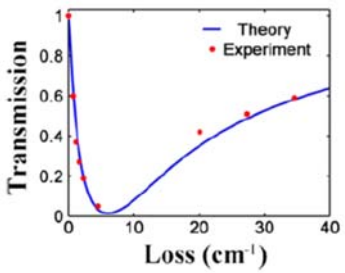

FIG. 4 (color online). Experimental observation of spontaneous passive $\mathcal{PT}$-symmetry breaking. Output transmission of a passive $\mathcal{PT}$ complex system as the loss in the lossy waveguide arm is increased. The transmission attains a minimum at 6 cm^{-1}.

PRL 103, 093902 (2009) PHYSICAL REVIEW LETTERS 28 AUGUST 2009

Observation of $\mathcal{PT}$-Symmetry Breaking in Complex Optical Potentials

A. Guo and G. J. Salamo
Department of Physics, University of Arkansas, Fayetteville, Arkansas 72701, USA

D. Duchesne and R. Morandotti
INRS-EMT, Varennes, Québec J3X 1S2, Canada

M. Volatier-Ravat and V. Aimez
Centre de Recherche en Nanofabrication et en Nanocaractérisation, Université de Sherbrooke, Sherbrooke, Québec J1K 2R1, Canada

G. A. Siviloglou and D. N. Christodoulides

Transverse $\mathcal{PT}$-symmetry

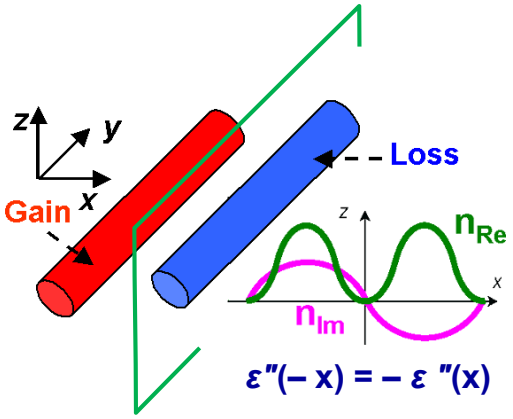

$\mathcal{PT}$-symmetry coupled waveguides

Longitudinal $\mathcal{PT}$-symmetry

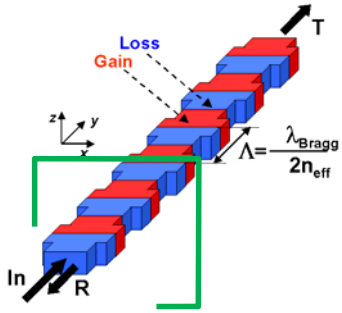

$\mathcal{PT}$-symmetry Bragg grating waveguide

PT-symmetry and Waveguides / (3) Waveguides & Bragg structures

Examples

- Waveguide based

- Just planar

Reminder : Ruter First (non-passive PT) demonstration is transverse PT

Christian E. Rüter[1], Konstantinos G. Makris[2], Ramy El-Ganainy[2], Demetrios N. Christodoulides[2], Mordechai Segev[3] and Detlef Kip[1]*

NATURE PHYSICS | VOL 6 | MARCH 2010 |

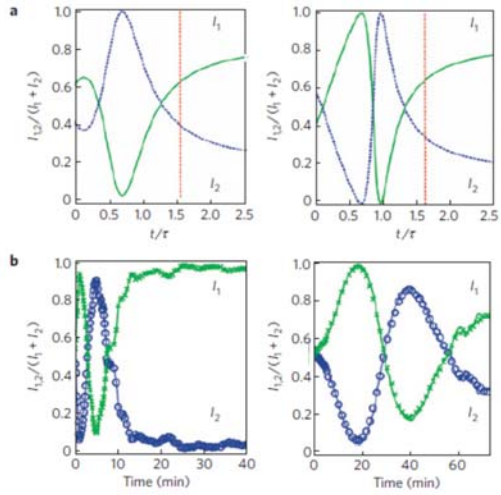

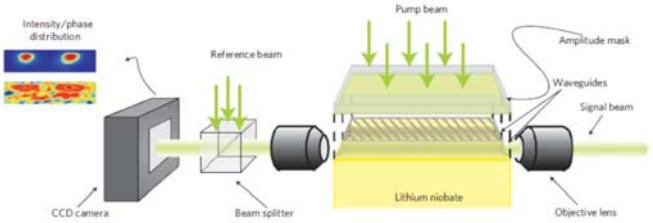

Figure 3 | Computed and experimentally measured response of a *PT*-symmetric coupled system. a, Numerical solution of the coupled equations (1) describing the *PT*-symmetric system. The left (right) panel shows the situation when light is coupled into channel 1 (2). Red dashed lines mark the symmetry-breaking threshold. Above threshold, light is predominantly guided in channel 1 experiencing gain, and the intensity of channels 1 and 2 depends solely on the magnitude of the gain. **b**, Experimentally measured (normalized) intensities at the output facet during the gain build-up as a function of time.

Experimental demonstration of a unidirectional reflectionless parity-time metamaterial at optical frequencies

NATURE MATERIALS j VOL 12 j FEBRUARY 2013 p.108

Liang Feng1*(, Ye-Long Xu2(,William S. Fegadolli1,3,4(, Ming-Hui Lu2*, José E. B. Oliveira3, Vilson R. Almeida3,4, Yan-Feng Chen2 and Axel Scherer1

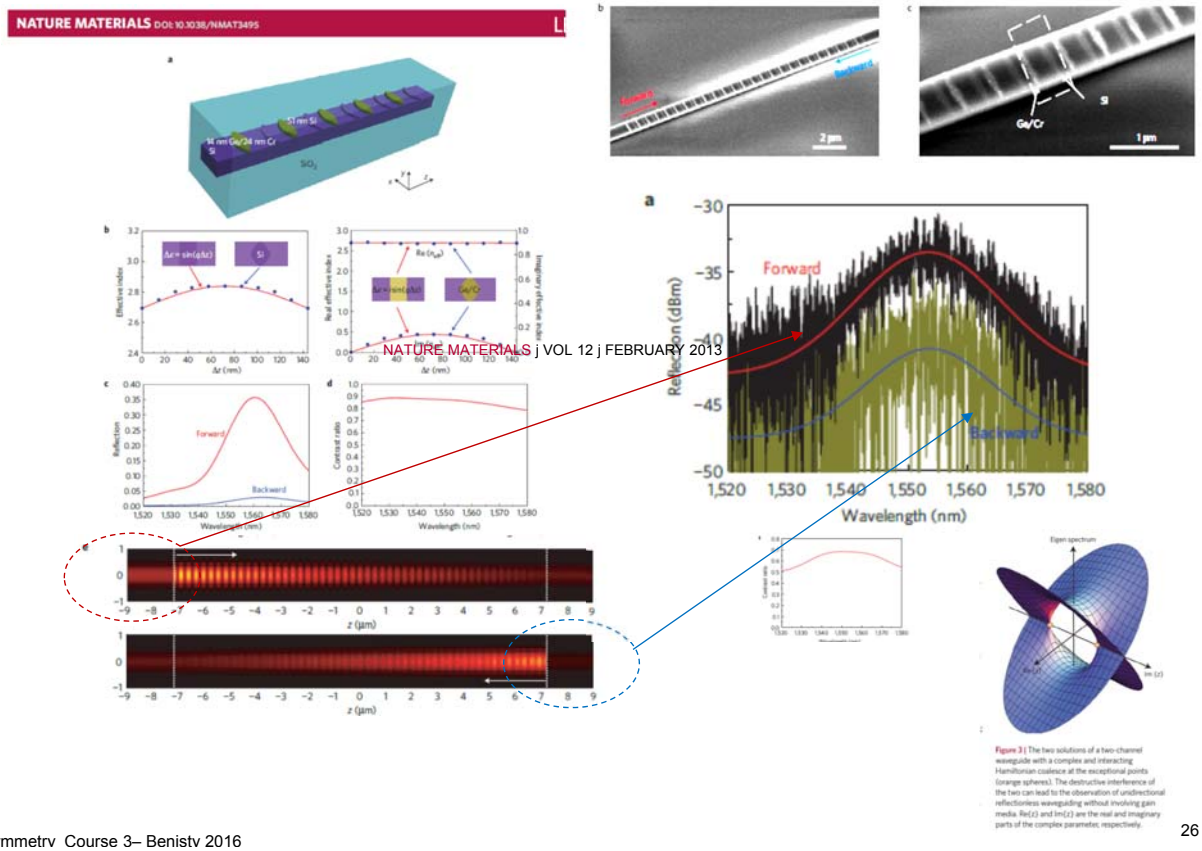

NATURE MATERIALS j VOL 12 j FEBRUARY 2013

Nonreciprocal Light Propagation in a Silicon Photonic Circuit

Liang Feng,[1,2,4*†] Maurice Ayache,[3*] Jingqing Huang,[1,4*] Ye-Long Xu,[2] Ming-Hui Lu,[2] Yan-Feng Chen,[2†] Yeshaiahu Fainman,[3] Axel Scherer[1,4†]

SCIENCE VOL 333 5 AUGUST 2011 729

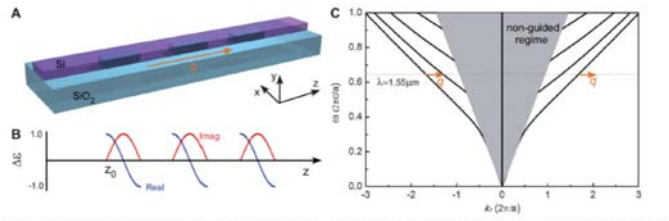

Fig. 1. (A) Nonreciprocal light propagation in a Si photonic circuit. Based on a SOI platform, PT optical potentials with exponentially modulated dielectric constants, as depicted in (B) where blue and red curves represent the real and imaginary parts of $\Delta\varepsilon$, respectively, are embedded in the Si waveguide to introduce an additional wave vector q to guided light. (C) Band diagram for TE-like polarization of the Si waveguide, where the frequency and wave vector are normalized with $a = 1\,\mu m$. At the wavelength of 1.55 μm, if incoming light is a fundamental symmetric mode, one-way mode conversion is only expected for backward propagation where the phase-matching condition is satisfied as indicated by arrows.

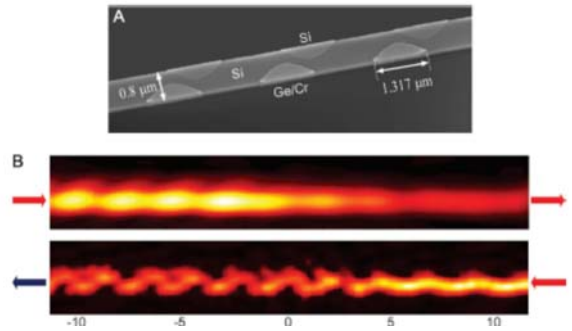

→ **Transition between two dispersion branches**

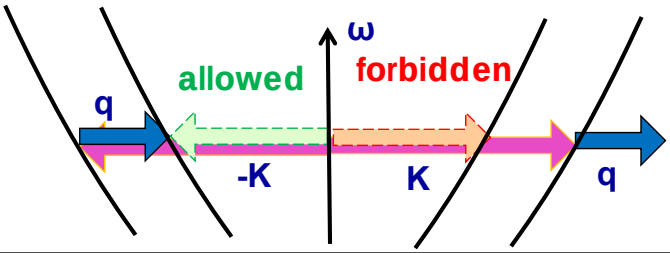

~~-K → -K-q~~

~~K → K-q~~

No -q!

Passive PT Symmetry in Organic Composite Films via Complex Refractive Index Modulation

***Multilayer passive* PT**

*Yixin Yan and Noel C. Giebink **

Adv. Optical Mater. **2014**,
DOI: 10.1002/adom.201400021

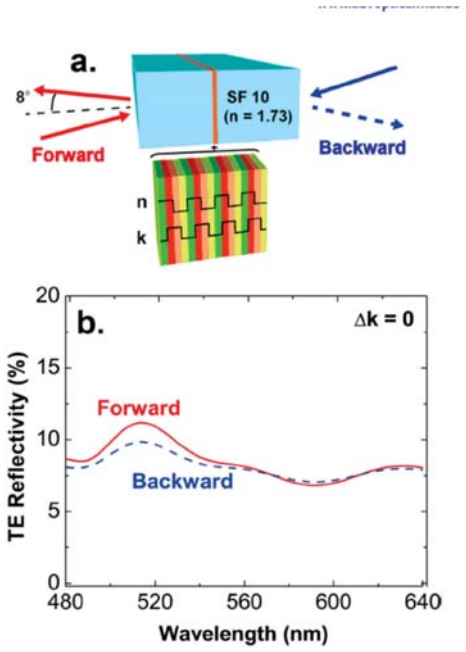

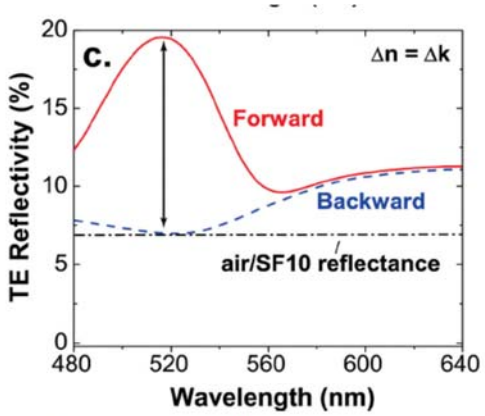

Figure 3. (a) Schematic of the CIM film and sample structure used for reflectivity measurements together with the discrete layer implementation of a complex exponential index profile. The forward and reverse incidence reflectivity spectra measured for samples with $\Delta k = 0$ and $\Delta k = \Delta n$ are shown in panels (b) and (c), respectively. In the latter case, a strong asymmetry in reflectivity is observed near the $\lambda = 532$ nm design wavelength and the internal reflectivity of the CIM film within the SF10 sandwich vanishes for reverse incident light.

Sliica / SI structures !

Multilayer passive PT

27 January 2014 | Vol. 22, No. 2 | DOI:10.1364/OE.22.001760 | OPTICS EXPRESS 1760

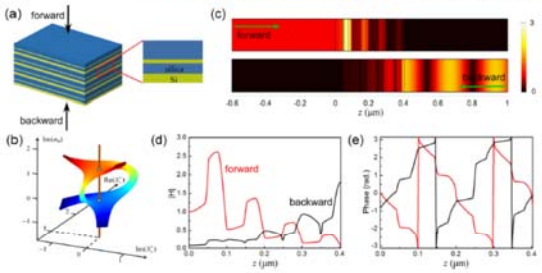

Fig. 1. (a) Schematic of the optical exceptional point structure on a glass wafer designed at the wavelength of 532 nm, where $n_{Si} = 4.86 - j0.65$ and $n_{silica} = 1.46$. (b) Complex eigen value solutions of the modified scattering matrix at 532 nm construct a multi-valued Riemann surface as a function of $\mathrm{Im}(n_a)$, where red color indicates optical gain and blue corresponds to absorption as we have in Si layers. (c) Simulations of light propagating through the exceptional point structure in the forward (upper panel) and backward (lower panel) directions, in which the distribution of the amplitude of the magnetic field is shown normalized to the incident magnetic field of 1. (d) and (e) are amplitude and phase of the magnetic field in the device as light propagate in the forward (red) and backward (black) directions, respectively.

Demonstration of a large-scale optical exceptional point structure

Liang Feng,[1] Xuefeng Zhu,[1,2] Sui Yang,[1,3] Hanyu Zhu,[1] Peng Zhang,[1] Xiaobo Yin,[1,3] and Yuan Wang,[1,3] and Xiang Zhang[1,3,*]

[1]National Science Foundation Nanoscale Science and Engineering Center, 3112 Etcheverry Hall, University of California, Berkeley, CA 94720, USA
[2]Huazhong University of Science and Technology, Wuhan, Hubei 430074, China
[3]Materials Sciences Division, Lawrence Berkeley National Laboratory (LBNL), 1 Cyclotron Road, Berkeley, CA

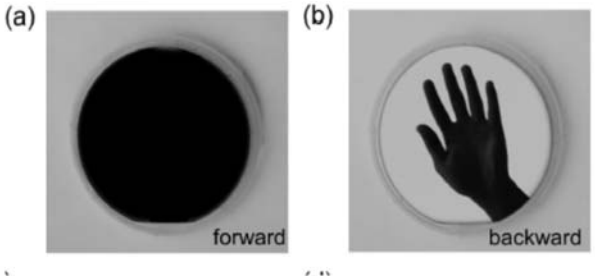

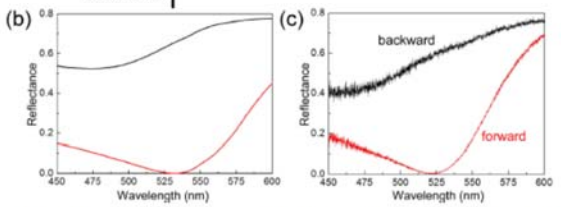

ig. 3. (a) SEM pictures of the cross-section of the fabricated exceptional point structure. Scale ar, 50 nm. (b) and (c) are numerically calculated and experimentally measured reflection pectra of the exceptional point structure from 450 nm to 600 nm, respectively, for both orward (red) and backward (black) incidence.

Temporal version of PT symmetry

doi:10.1038/nature11298

Parity–time synthetic photonic lattices

Alois Regensburger[1,2], Christoph Bersch[1,2], Mohammad-Ali Miri[3], Georgy Onishchukov[2], Demetrios N. Christodoulides[3] & Ulf Peschel[1]

9 AUGUST 2012 | VOL 488 | NATURE | 167

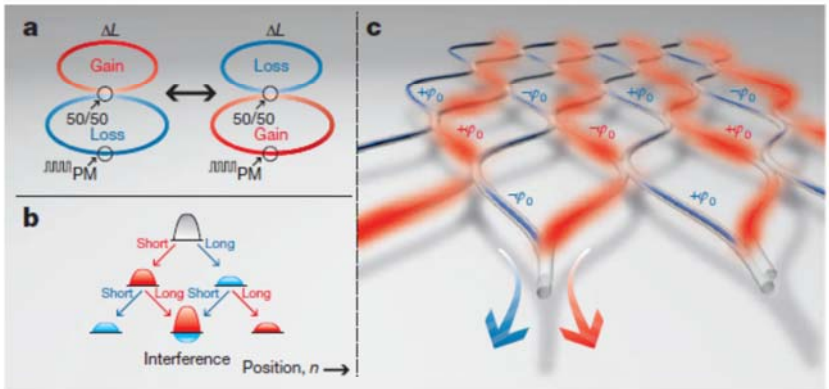

Figure 1 | PT-symmetric fibre networks. a, Two coupled fibre loops periodically switching between gain and loss as used in the experiment (Supplementary Fig. 1). Pulses are delayed or advanced as a result of a length difference ΔL between the loops. PM, phase modulator. b, Pulse evolution in the networks. Passages through short and long loops are indicated. c, Equivalent PT-symmetric lattice network. Gain (red) and loss (blue) channels are positioned antisymmetrically and are periodically coupled. Moreover, the real part of the potential is evenly imposed by phase shifts $\pm\varphi_0$.

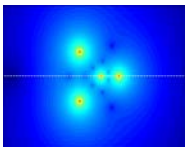

- Course 3 :
  - Bragg with gain/loss (complex ε) modulation
  - Unidirectionality of plane-wave coupling
  - **History of gain-modulation (1970's & 1990's)**
  - Kulishov's proposals :
    single-sided mirrors, strange cavities, memories
  - WGM lasers
  - Fano & EIT

Historical 1972 Kogelnik&Shank CMT paper : already gain DFB is there

Coupled-Wave Theory of Distributed Feedback Lasers

H. Kogelnik and C.V. Shank J. Appl. Phys., Vol. 43, No. 5, May 1972

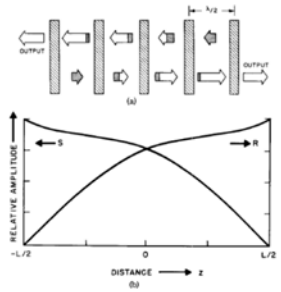

FIG. 1. (a) Illustration demonstrating laser oscillation in a periodic structure. (b) Plot of the amplitudes of left traveling wave S and right traveling wave R vs distance.

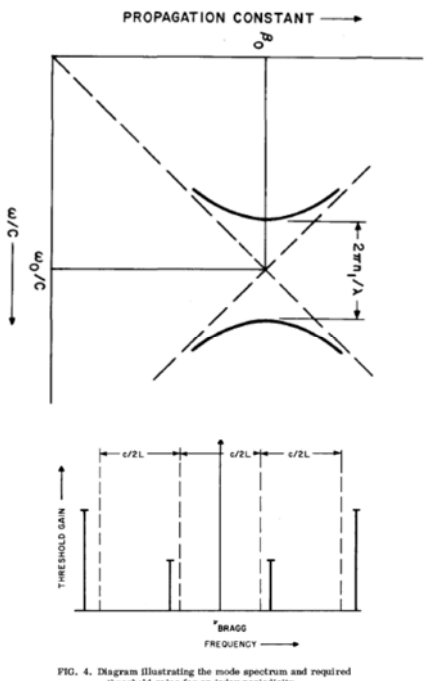

FIG. 4. Diagram illustrating the mode spectrum and required threshold gains for an index periodicity.

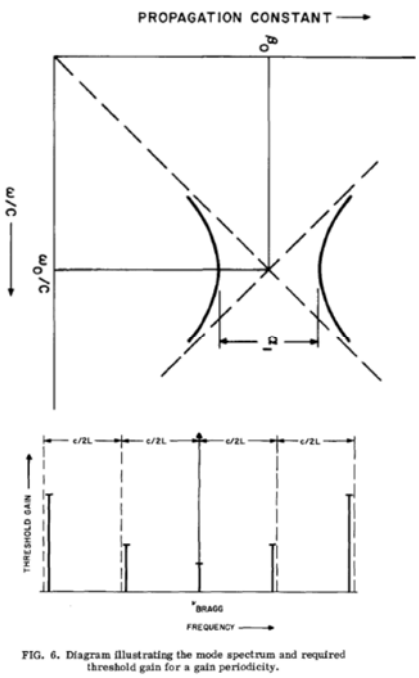

FIG. 6. Diagram illustrating the mode spectrum and required threshold gain for a gain periodicity.

sion spot. Effects of rigid refractive index and gain-loss profiles built into the laser crystal on the mode stability have been examined, and conditions for kink-free, single lateral mode oscillations have been investigated.

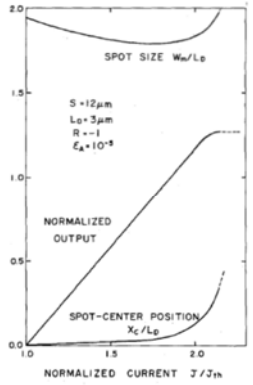

Fig. 2. Solid lines are calculated current dependence of output, emission spot size, and spot-center position.

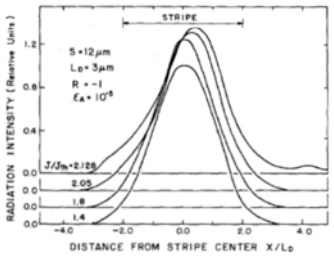

Fig. 3. Calculated near-field intensity profiles at different current levels corresponding to Fig. 2.

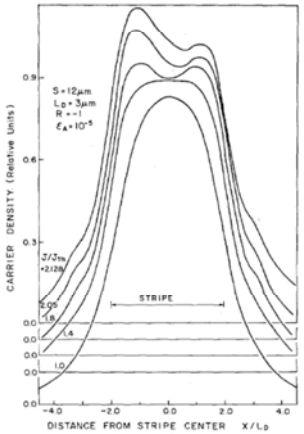

Fig. 4. Calculated carrier density profiles at different current levels corresponding to Fig. 2.

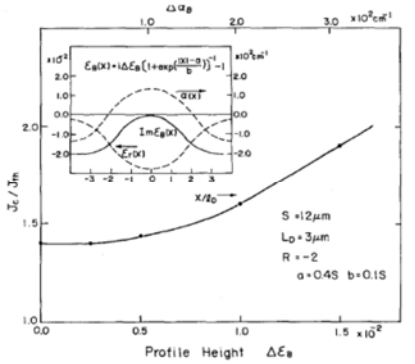

Fig. 9. Dependence of the critical current density on the built-in profile height $\Delta\varepsilon_B$ of the imaginary dielectric constant ($\Delta\alpha_B$ of loss). The assumed profile shape is shown in the inset. Other notations are the same as those in Fig. 8.

Purely gain-coupled distributed feedback semiconductor lasers

Y. Luo,[a] Y. Nakano,[b] and K. Tada[a]
University of Tokyo, 7-3-1 Hongo, Bunkyo-ku, Tokyo 113, Japan
T. Inoue, H. Hosomatsu, and H. Iwaoka
Optical Measurement Technology Development Co., Ltd., 2-11-13 Naka-cho, Musashino-shi, Tokyo 180, Japan

1620 Appl. Phys. Lett. 56 (17), 23 April 1990

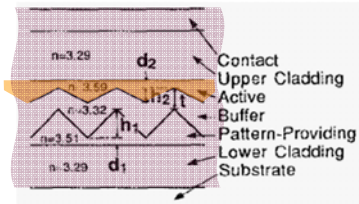

FIG. 1. Schematic drawing of the longitudinal cross section of the new DFB laser structure for pure gain coupling.

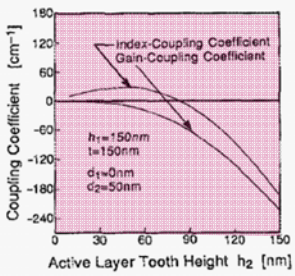

FIG. 2. Gain- and index-coupling coefficients for a second-order symmetric triangular grating.

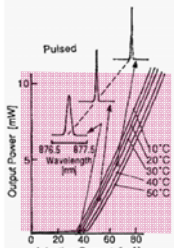

FIG. 4. Light output vs current characteristics and emission spectra at several injection levels.

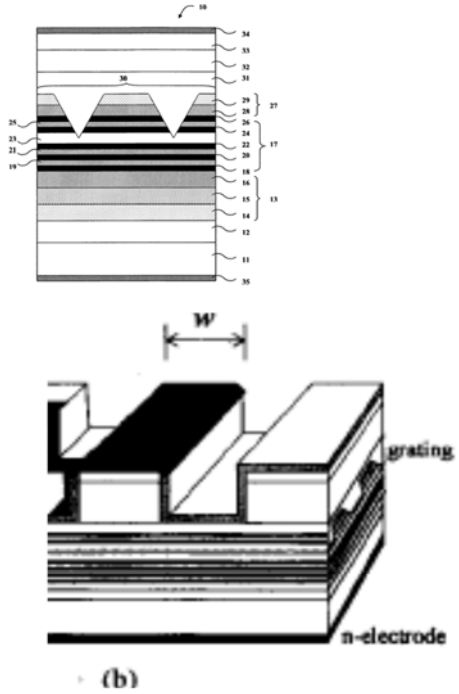

JOURNAL OF LIGHTWAVE TECHNOLOGY, VOL. 13, NO. 2, FEBRUARY 1995
196

Multi-λ Ridge Waveguide Gain-Coupled DFB Laser Array

G. P. Li, T. Makino, *Member, IEEE*, and C. M. Wu

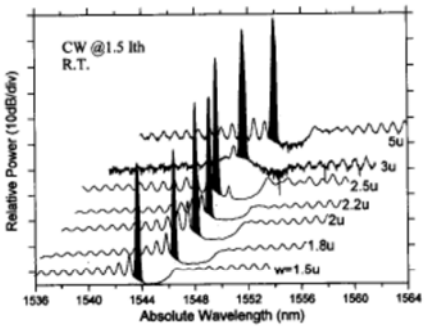

Fig. 3. Lasing spectra of 7 element lasers in the array at cw I_{th}, 20°C. (w = ridge width).

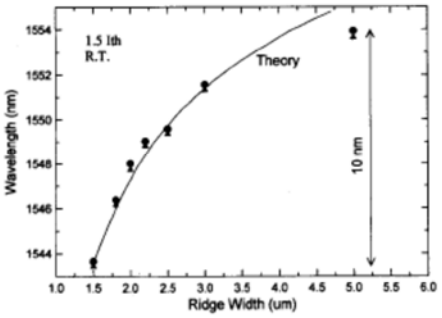

Fig. 4. Ridge width dependence of lasing wavelengths at 1.5 I_{th} and 20°C. The closed circles are the results of cw and triangles are those for the pulse (T: 10 ms; Duty: 0.8 ms) operations, respectively. The solid curve shows theoretical results.

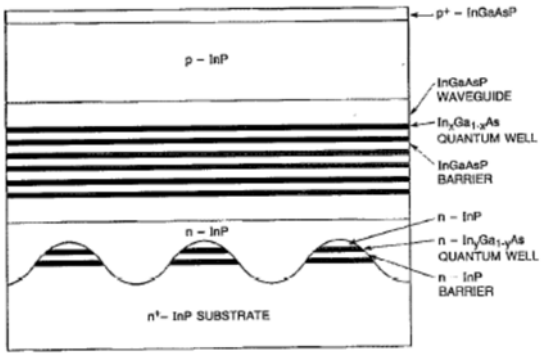

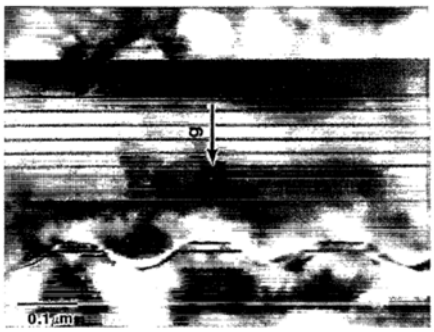

FIG. 2. A TEM photograph of the cross-sectional view of a 6-QW $In_{0.6}Ga_{0.4}As$ (5 nm)/$Q_{1.25}$ (18.6 nm) active-layer DFB laser with a 2-QW $In_{0.62}Ga_{0.38}As$ (4 nm)/InP (9.3 nm) grating.

Semiconductor distributed feedback lasers with quantum well or superlattice gratings for index or gaincoupled optical feedback

W. T. Tsang, F. S. Choa, M. C. Wu, Y. K. Chen, R. A. Logan, S. N. G. Chu, A. M. Sergent, and C. A. Burrus

Citation: Applied Physics Letters **60**, 2580 (1992); doi: 10.1063/1.106915

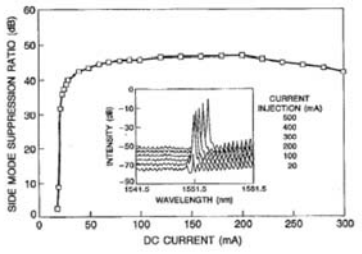

FIG. 5. The SMSR as a function of injection current. The inset shows the spectra at different injection currents. Near threshold the DFB mode is relatively well centered with a small Bragg stop band.

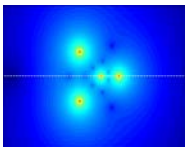

- Course 3 :
  - Bragg with gain/loss (complex ε) modulation
  - Unidirectionality of plane-wave coupling
  - History of gain-modulation (1970's & 1990's)
  - **Kulishov's proposals : single-sided mirrors, strange cavities, memories**
  - WGM lasers

Fig. 1. General structure of an amplifying tunable filter based on (a) grating-assisted codirectional coupler and (b) long-period fiber grating.

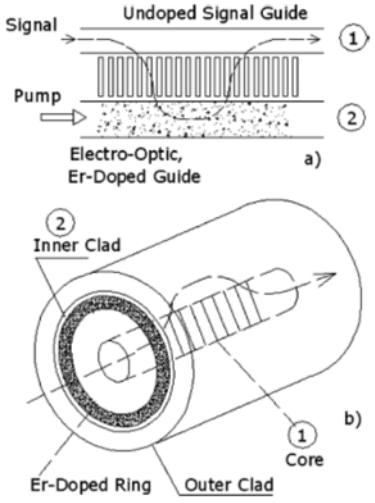

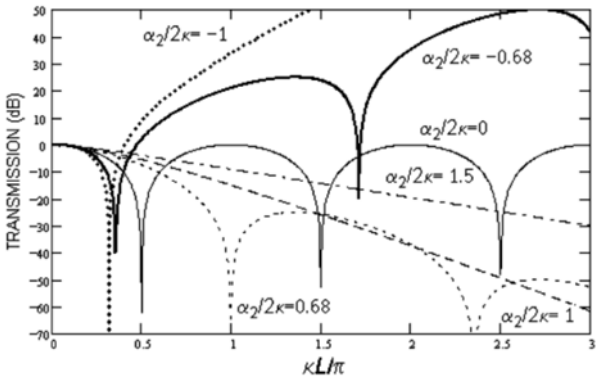

Variation of the grating transmission at the resonance wavelength with the grating strength κL for different gain/loss parameter values.

First clear (theoretical) occurrence of Bragg nonreciprocal grating in optics

Nonreciprocal waveguide Bragg gratings

Mykola Kulishov [a, b], Jacques M. Laniel [a], Nicolas Bélanger [a], José Azaña [c], David V. Plant [a]

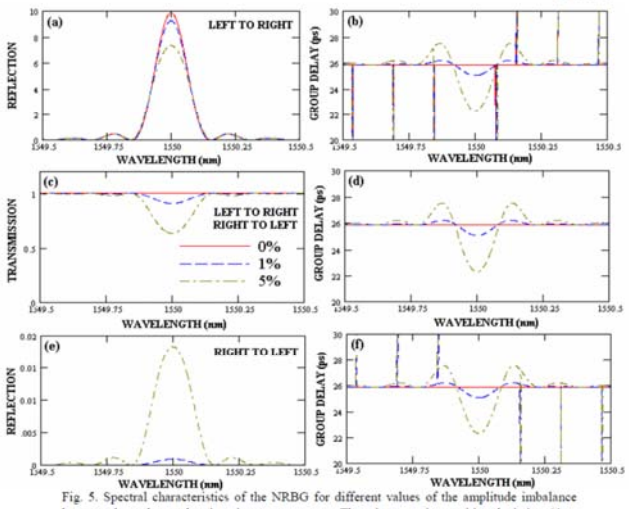

Fig. 5. Spectral characteristics of the NRBG for different values of the amplitude imbalance between the real κ_n and κ_α imaginary components. There is no grating position deviation ($\Delta z = 0$): (a) reflection spectrum and (b) reflection group delay for light launched into the left side of the grating ($z = 0$); (c) transmission spectrum and (d) transmission group delay (the transmission characteristics are the same regardless the light input direction, $z = 0$ or L); (e) reflection spectrum and (f) reflection group delay for light injected into the right side of the grating ($z = L$).

$$\kappa_{12} = \left[\kappa_n - \kappa_\alpha \exp\left(j\,2\pi\Delta z/\Lambda\right)\right],$$
$$\kappa_{21} = \left[\kappa_n + \kappa_\alpha \exp\left(-\,j\,2\pi\Delta z/\Lambda\right)\right].$$

18 April 2005 / Vol. 13, No. 8 / OPTICS EXPRESS 3068

Use of Four-port devices, with memory in a loop

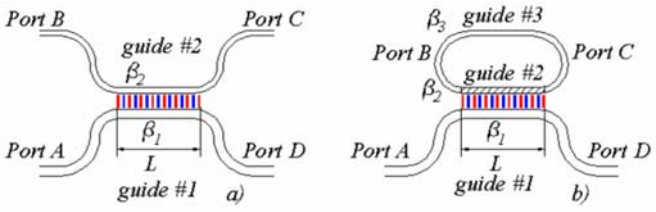

Trapping light in a ring resonator using a grating-assisted coupler with asymmetric transmission

Mykola Kulishov [a, b], Jacques M. Laniel [a], Nicolas Bélanger [a], David V. Plant [a]

2 May 2005 / Vol. 13, No. 9 / OPTICS EXPRESS 3567

New cavity concept : PT mirrors from inside …

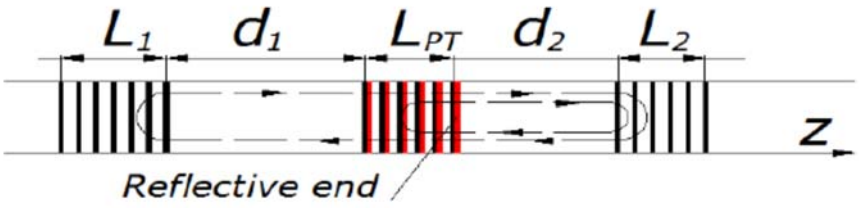

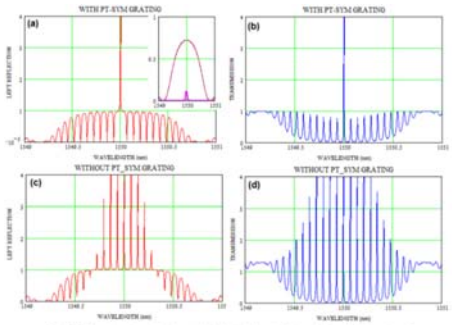

Fig. 2. Fully constructive interference: left reflection (a, c) and transmission (b, d) spectra of the DBG FP resonator with the PT-SBG grating inside the cavity and of the DBR FP resonator without PTSB (b, d) and with an amplifying waveguide ($\alpha = -12$ μm^{-1}). The structure parameters are: $\Delta = 0.5$ μm; $L_1 = L_2 = 2000\Delta$ = 1 mm; $\kappa_1 = \kappa_2 = 125$ m^{-1}; $L_{PT} = 20000\Delta$=10000 μm; κ_{PT} =32.67 m^{-1}; d_1 = 100Λ = 50 μm ; d_2 =1000.5Δ=500.25 μm. The insert in (a) shows the reflection spectra of the left (blue), right (red) and PT-symmetric Bragg grating (magenta).

http://arxiv.org/ftp/arxiv/papers/1505/1505.01391.pdf

Unique optical characteristics of a Fabry-Perot resonator with embedded *PT*-symmetrical grating

Mykola Kulishov,[1,*] Bernard Kress,[2] and H. F. Jones[3]

Angular study of more complex gratings…

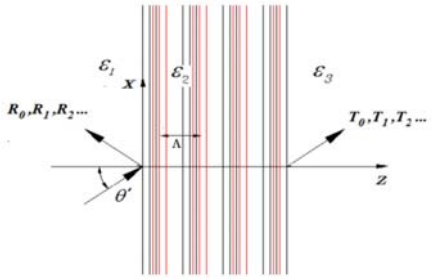

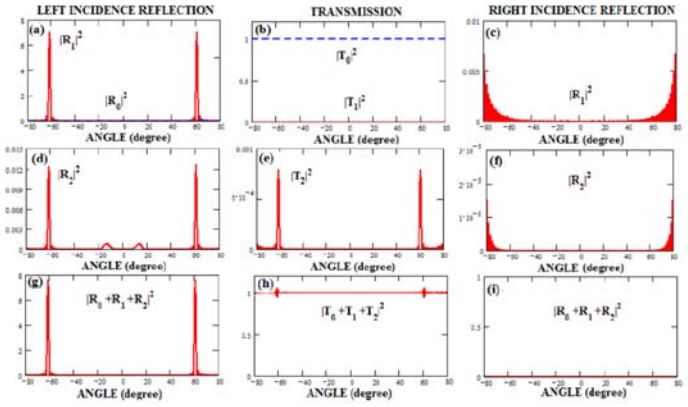

http://arxiv.org/ftp/arxiv/papers/1505/1505.01391.pdf

Analysis of unidirectional non-paraxial invisibility of purely reflective *PT*-symmetric volume gratings

Mykola Kulishov,[1*] H.F. Jones,[2] and Bernard Kress[3]

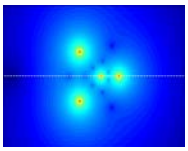

- Course 3 :
  - Bragg with gain/loss (complex ε) modulation
  - Unidirectionality of plane-wave coupling
  - History of gain-modulation (1970's & 1990's)
  - Kulishov's proposals :
    single-sided mirrors, strange cavities, memories
  - **WGM lasers**
  - Fano & EIT

Coupled Laser studies related to PT symmetry

(beyond the caveat « infinite transmission »)

PRL 108, 173901 (2012)

M. Liertzer,[1,*] Li Ge,[2] A. Cerjan,[3] A. D. Stone,[3] H. E. Türeci,[2,4] and S. Rotter[1,†]

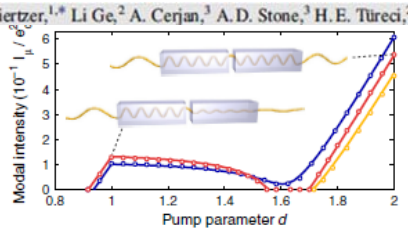

FIG. 1 (color online). Intensity output of a laser system consisting of two 1D coupled ridge lasers, each of length 100 μm with an air gap of size 10 μm and an (unpumped) index of refraction $n = 3 + 0.13i$. For $0 < d < 1$, the pump in the left ridge is linearly increased in the range $0 < D < 1.2$, and, for

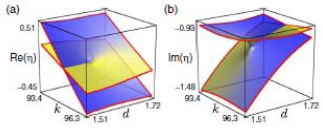

Stefano Longhi

PRL 105, 013903 (2010) PHYSICAL REV

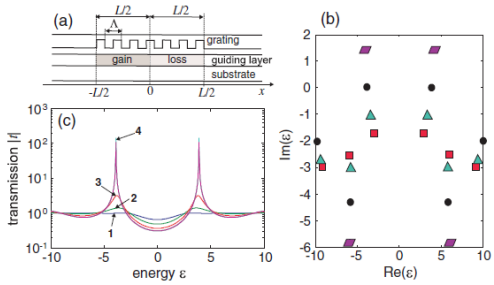

Non-Hermitian Dirac equation and its optical realization.—Let us consider the Dirac equation in one spatial

Won-Tien Tsang, one of the three inventors of the cleaved coupled-cavity laser, prepares

Bell Lab patent 1965
Tsang 1984
C3 laser
(Coupled cavity laser)

Conceptually, the simplest case of PT-symmetry !?

Symmetry-breaking scanned by means of Variable Coupling

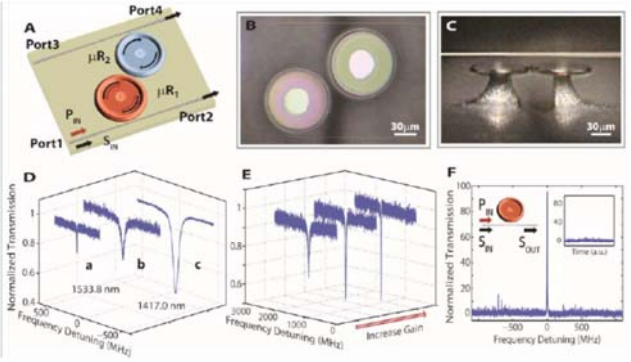

Fig.1. Concept of the PT-symmetric WGM microcavities. (A) The system consists of two directly coupled WGM resonators, and two fiber-taper waveguides. μR_1: active Er^{3+}-doped silica microtoroid. μR_2: passive silica microtoroid. P_{IN}: pump laser in 1460 nm band to excite Er^{3+} ions which provide gain in the 1550 nm band. S_{IN}: probe light (signal) in the 1550 nm band.

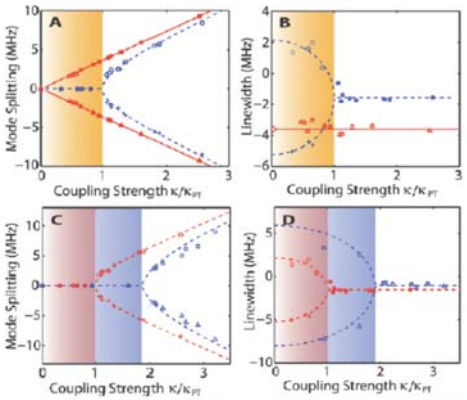

Fig.2. Experimentally observed mode-splitting and linewidth-difference of the supermodes in the coupled-microresonator system as a function of coupling strength κ. *Mode-splitting **(A&C)** and linewidth **(B&D)** variation correspond to the difference between the real parts and changes in the imaginary parts of the eigenfrequencies, respectively. **(A&B)** Comparison when resonators are passive (no gain in μR_1: red square and triangular marks) with Q factors 2.9×10^7 and 3.0×10^7, respectively, for μR_1 and μR_2, and when one resonator is active and the other is passive (with gain in μR_1: blue circular and cross marks). **(C&D)** Effect of the initial Q-factor (loss) of μR_2 on the eigenfrequencies. Two resonance modes with Q-factors 2.0×10^7 (blue) and 3.0×10^7 (red) are chosen for μR_2. Shaded regions correspond to the broken-PT-symmetric region when gain and loss are balanced.*

PT-symmetry and Waveguides / (1) Waveguides & Bragg structures

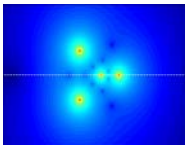

- Course 3 :
  - Bragg with gain/loss (complex ε) modulation
  - Unidirectionality of plane-wave coupling
  - History of gain-modulation (1970's & 1990's)
  - Kulishov's proposals : single-sided mirrors, strange cavities, memories
  - WGM lasers
  - **Fano & EIT**

The all-pass filter, aka « Gire-Tournois etalon »,…

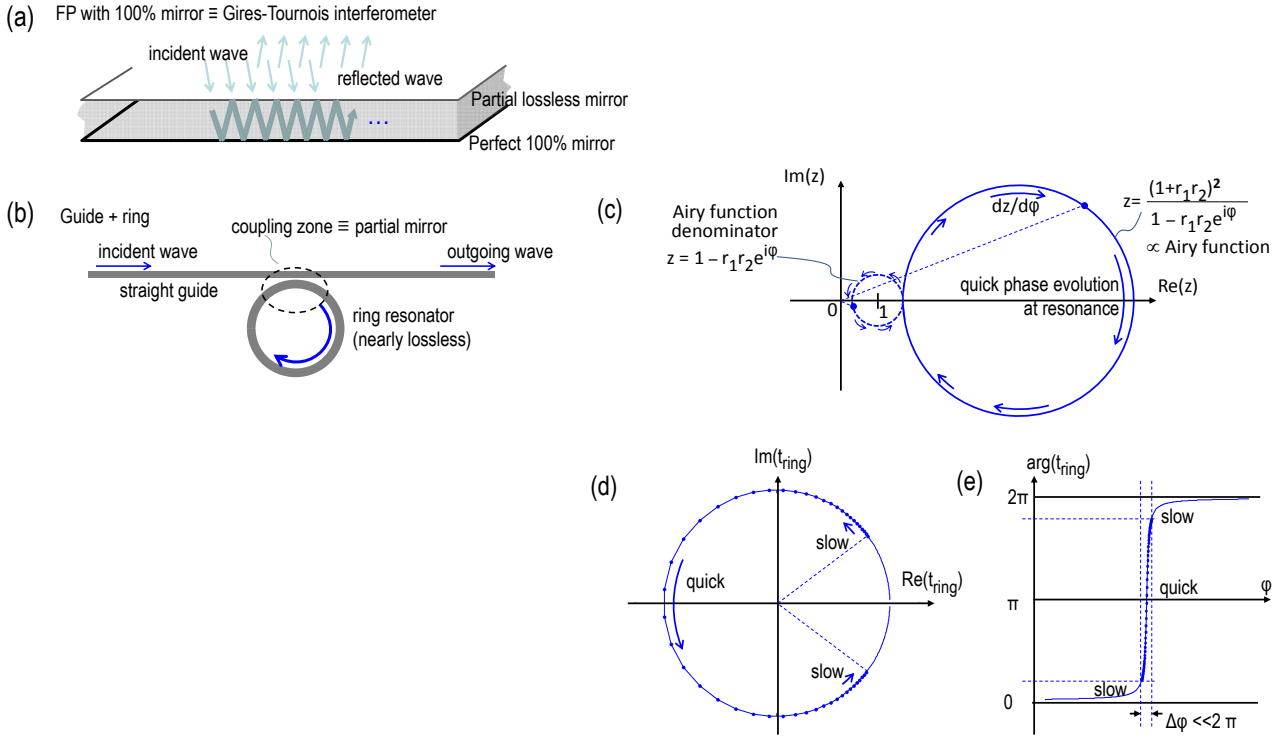

Fano = 3 continuum ports + 1 resonance

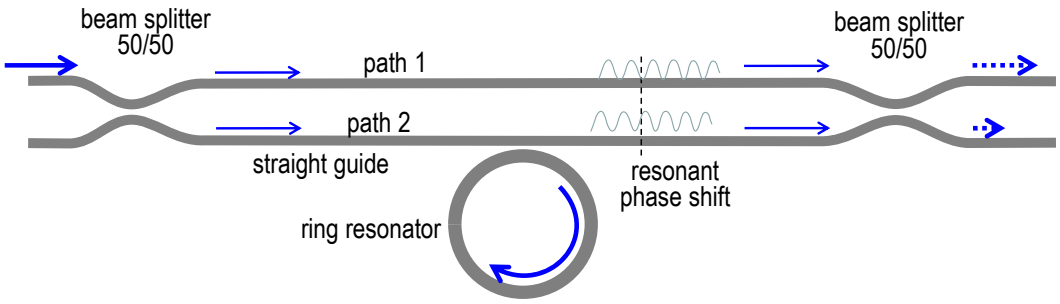

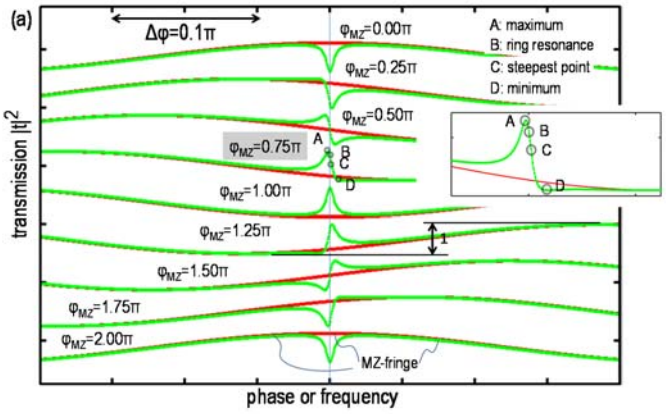

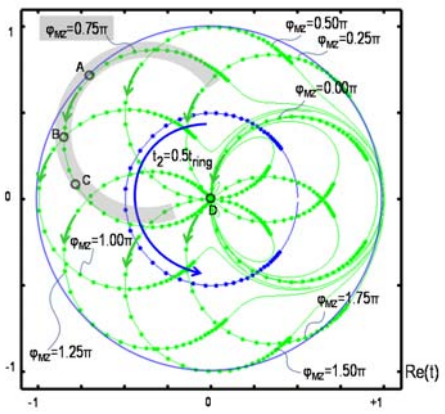

Fano ← Resonant waveguide grating

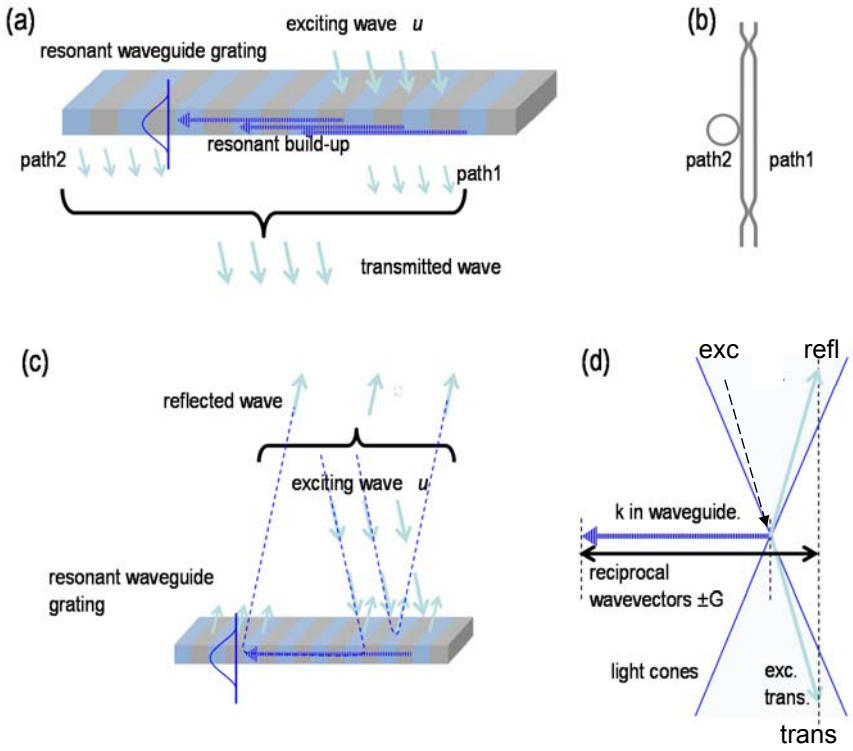

Fano, Poles picture and CMT

Bridging pole and coupled wave formalisms for grating waveguide resonance analysis and design synthesis

*Pietroy et al. OE , **15**, 9831, 2007*

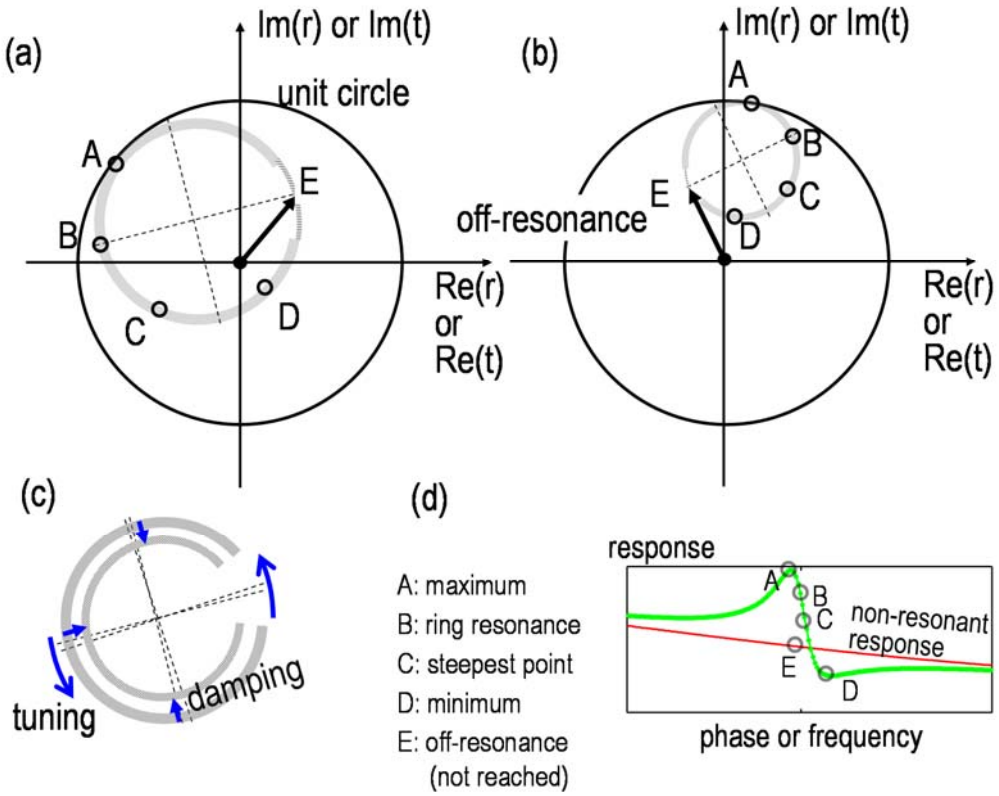

EIT (Electromagnetically Induced Transparency)

(historically: a linear phenomenon of atom physics
…albeit a nonlinear optical phenomenon : lasers intensities are coupling constants for atoms)

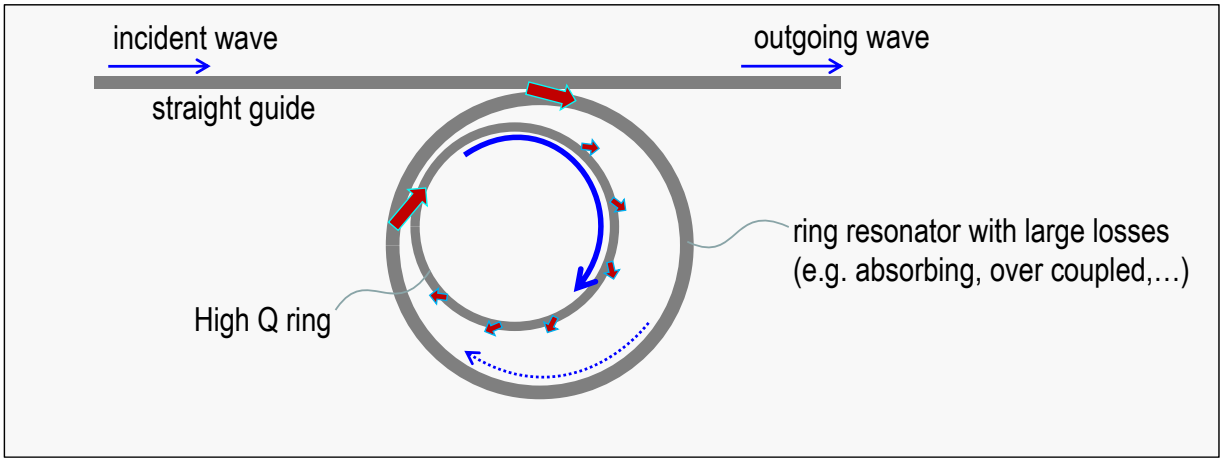

KEY ? equal transfers across lossy resonator: 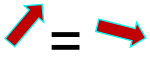

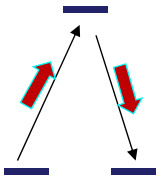

PT-symmetry and Waveguides / (3) Waveguides & Bragg structures

Conclusion

••• *Microscopic view of Reflectivity-**asymmetry** in basic PT-symmetric Bragg structures*

••• *Many possible implementations investigated (planar, guided, organics, semiconductors)*

••• *Trove of concepts*
-from « PT outsiders », (e.g. Kulishov)
- from metamaterials (here e.g. Jensen Li)
- Around lasing and coupled lasers
(thus good scientific « friction »)